

FedCanon: Non-Convex Composite Federated Learning with Efficient Proximal Operation on Heterogeneous Data

Yuan Zhou, Jiachen Zhong, Xinli Shi, *Senior Member, IEEE*,
Guanghui Wen, *Senior Member, IEEE*, and Xinghuo Yu, *Fellow, IEEE*

Abstract—Composite federated learning offers a general framework for solving machine learning problems with additional regularization terms. However, many existing methods require clients to perform multiple proximal operations to handle non-smooth terms and their performance are often susceptible to data heterogeneity. To overcome these limitations, we propose a novel composite federated learning algorithm called FedCanon, designed to solve the optimization problems comprising a possibly non-convex loss function and a weakly convex, potentially non-smooth regularization term. By decoupling proximal mappings from local updates, FedCanon requires only a single proximal evaluation on the server per iteration, thereby reducing the overall proximal computation cost. It also introduces control variables that incorporate global gradient information into client updates, which helps mitigate the effects of data heterogeneity. Theoretical analysis demonstrates that FedCanon achieves sublinear convergence rates under general non-convex settings and linear convergence under the Polyak-Łojasiewicz condition, without relying on bounded heterogeneity assumptions. Experiments demonstrate that FedCanon outperforms the state-of-the-art methods in terms of both accuracy and computational efficiency, particularly under heterogeneous data distributions.

Index Terms—Federated Learning, Non-convex Composite Optimization, Convergence Rate, Data Heterogeneity.

I. INTRODUCTION

Traditional machine learning often relies on aggregating data for model training, which may raise significant privacy concerns and incur high communication costs, particularly for large-scale learning tasks [1]. To address these challenges, Federated Learning (FL) has been proposed [2], with Federated Averaging (FedAvg) [3] being one of the most commonly utilized frameworks. In FedAvg, multiple clients collaboratively train a global model under the coordination of a central server, without sharing their local datasets. The framework allows clients to perform multiple rounds of local training before communication. By effectively leveraging distributed devices, preserving privacy, and reducing communication overhead, FL

has achieved significant progress in fields such as computer vision, natural language processing, and statistical analysis [1], [4]–[6].

Most of the current research on FL focuses on unconstrained and smooth objective problems. However, to ensure that the obtained solutions possess desirable properties such as sparsity or low rank, additional regularization terms are often required [7]–[9]. This leads to the following composite FL formulation:

$$\min_{z \in \mathbb{R}^d} \phi(z) = f(z) + h(z), \quad f(z) \triangleq \frac{1}{N} \sum_{i=1}^N f_i(z), \quad (1)$$

where $z \in \mathbb{R}^d$ is model parameter, N denotes the number of clients participating in the training, f_i is the local loss function, and h is a possibly non-smooth regularization term. For the composite optimization problem (1), the most commonly used algorithm is Proximal Gradient Descent (PGD), which is a forward-backward splitting method [10]–[12]:

$$z^{t+1} = \text{prox}_{\alpha h} \{z^t - \alpha \nabla f(z^t)\}, \quad t = 0, \dots, T-1, \quad (2)$$

where $\text{prox}_{\alpha h} \{y\} = \arg \min_x \{h(x) + \frac{1}{2\alpha} \|x - y\|^2\}$ represents the proximal operator associated with the regularization term h , and $\alpha > 0$ is the step size. Although the proximal operator essentially involves solving another optimization problem, many commonly used regularization terms have well-established closed-form solutions. When adapted to the FL paradigm, PGD naturally leads to the following formulation:

$$\hat{x}_i^{t,0} = z^t, \quad \hat{x}_i^{t,k+1} = \text{prox}_{\beta h} \{\hat{x}_i^{t,k} - \beta g_i(\hat{x}_i^{t,k})\}, \quad (3a)$$

$$\bar{\Delta}^t = \frac{1}{N} \sum_{i=1}^N \Delta_i^t = \frac{1}{N} \sum_{i=1}^N \left(z^t - \hat{x}_i^{t,K} \right), \quad (3b)$$

$$z^{t+1} = \text{prox}_{\alpha h} \{z^t - \alpha \bar{\Delta}^t\}, \quad (3c)$$

where $\hat{x}_i^{t,k}$ represents the local model, and $g_i(\hat{x}_i^{t,k})$ is the unbiased and variance-bounded stochastic gradient. The above (3a) corresponds to the local updates of client i for $k = 0, \dots, K-1$. Meanwhile, the server also maintains the global gradient z^t , which is broadcast at the start of the local updates. Afterwards, the server uses the aggregated result from (3b) to replace the gradient $\nabla f(z^t)$ in (2) and update the global model in (3c). Essentially, (3) extends FedAvg by incorporating proximal operator, while also serving as a special case of FedMiD in [8]. However, directly using (3) to solve problem (1) may lead to the following three potential issues.

First, the information aggregated by the server includes the post-proximal states of the local clients. Since proximal

Yuan Zhou and Jiachen Zhong are with the School of Cyber Science and Engineering, Southeast University, Nanjing 210096, China (e-mail: zhouxyz@seu.edu.cn; jiachen_zhong@seu.edu.cn).

Xinli Shi is with the School of Cyber Science and Engineering, Southeast University, Nanjing, China, 210096, and also with the School of Engineering, RMIT University, Melbourne, VIC 3001, Australia. (e-mail: xinli_shi@seu.edu.cn).

Guanghui Wen is with the School of Automation, Southeast University, Nanjing 210096, China (e-mail: ghwen@seu.edu.cn).

Xinghuo Yu is with the School of Engineering, RMIT University, Melbourne, VIC 3001, Australia (e-mail: x.yu@rmit.edu.au).

TABLE I
TIME COST (MILLISECOND) OF A SINGLE PROXIMAL MAPPING FOR
VARIOUS REGULARIZATION TERMS ON DIFFERENT NEURAL NETWORKS

Models	ℓ_1 -norm	MCP	SCAD penalty
MLP	0.3	1	3
CNN	4	8	19
ResNet-18	134	255	636
ResNet-102	672	1221	2537

All elements in the table are tested on the same device, with the MNIST dataset. The model size increases from top to bottom. ‘‘MCP’’ refers to Minimax Concave Penalty, and ‘‘SCAD’’ refers to Smoothly Clipped Absolute Deviation.

mappings are typically nonlinear, the local update equations in (3b) cannot be telescoped as in FedAvg to extract the gradient $\frac{1}{NK} \sum_{i=1}^N \sum_{k=0}^{K-1} g_i(\hat{x}_i^{t,k})$ [13]. Moreover, as pointed out in [8], if h is the ℓ_1 -norm, the proximal mapping on local clients (corresponding to the soft-thresholding function in this case) induces sparsity in the local models. However, upon aggregation on the server, the resulting values may lose their sparsity, a phenomenon referred to as the ‘‘curse of primal averaging’’ [8]. To address this, [8] proposes an FL algorithm based on Dual Averaging, where the dual states are aggregated. Meanwhile, the algorithm in [13] (denoted as ZA1) decouples the proximal operator from communication and requires clients to directly transmit the pre-proximal local models. These allow the server to recover the gradient information effectively.

Furthermore, both local and global model updates involve significant proximal mapping computations. In one outer iteration of (3), each client needs to perform K local proximal mappings, in addition to the single proximal mapping executed by the server. Similar issue occurs in other works in composite FL, such as [4], [8], [13]. Although many commonly used regularization terms have fixed and known proximal mappings, this does not necessarily imply computational efficiency. In TABLE I, we compare the time required to perform a single proximal mapping for four neural network models with different sizes. It is evident that as the complexity of the proximal mapping increases and the neural network size grows, the time spent handling the regularization term becomes significant and cannot be overlooked. Fortunately, [14] also consider this issue and proposes ProxSkip, which allows for optionally skipping the proximal mapping step following a gradient descent step, providing critical inspiration for the subsequent research, though it is designed for centralized settings.

Finally, due to the distributed storage nature of FL, data heterogeneity is inevitable, often manifesting as label skew, feature skew, and quantity skew, among others [5], [6], [15], [16]. This heterogeneity can cause significant divergence among local models after several rounds of updates, negatively impacting the convergence rate and training accuracy of the aggregated global model, a phenomenon known as ‘‘client drift’’ [17]–[19]. Many FL methods, including FedAvg [19], [20], rely on the assumption that the heterogeneity of data is controllable, meaning that the gradient difference between the local and global loss functions is bounded [21]–[23]. This assumption appears in various forms, as detailed in Section III-A. To address this issue, clients can incorporate global gradient information into their local updates [14], [19], or

introduce penalty terms to prevent excessive divergence of local models [24], [25].

Contributions. This work aims to address the above issues by proposing a novel non-convex composite FL method with efficient proximal operation. We summarize our contributions as follows:

- **A General and Efficient FL method for Non-convex Composite Optimization with Data Heterogeneity.** We propose a composite Federated learning algorithm with efficient proximal operations and the ability to address data heterogeneity (FedCanon). This algorithm could simultaneously resolve the three aforementioned problems, and has the following advantages:
 - **Generality.** It addresses a general non-convex composite optimization problem, where the loss function can be non-convex, and the regularization term is weakly convex and possibly non-smooth. Unlike many existing methods, our algorithm does not rely on strong assumptions such as strong convexity, bounded gradients or bounded heterogeneity.
 - **Efficient Proximal Operation.** It eliminates the need for any proximal operations on local updates of clients. Instead, each iteration performs a single proximal mapping solely on the server, substantially reducing the overall computational cost. To the best of our knowledge, this is the first application of the proximal-skipping idea in non-convex composite FL.
 - **Robust to Data heterogeneity.** By introducing control variables, local updates on clients utilize global gradient information, effectively mitigating the impact of data heterogeneity. This contributes to a relatively underexplored area, as few existing composite FL methods explicitly account for data heterogeneity.
- **Explicit Convergence Rate.** Without any bounded heterogeneity assumptions, we demonstrate that the proximal gradient of the algorithm decreases at a sublinear rate of $\mathcal{O}(1/T)$ under a general non-convex objective assumption, until reaching a steady-error. If the objective function further satisfies a more general form of Polyak-Łojasiewicz (PL) condition, FedCanon converges linearly to a neighborhood of the optimal solution. All the convergence analyses require no extra convexity conditions on the objective function.
- **Comprehensive Numerical Experiments.** We apply FedCanon to real neural networks and training datasets, and compare its performance with several state-of-the-art FL methods. Experimental results show that, FedCanon effectively handles proximal operations under heterogeneous data distributions, achieving shorter training time and higher accuracy, thereby validating its effectiveness.

Notation. In the paper, we symbolize the d -dimensional vector space as \mathbb{R}^d and use $\mathbf{0}_d$ to represent a d -dimensional zero vector. The ℓ_1 -norm and ℓ_2 -norm are denoted by $\|\cdot\|_1$ and $\|\cdot\|$, respectively. We use $[N]$ to represent the set $\{1, \dots, N\}$. The differential operator is denoted by ∇ , the subdifferential operator by ∂ , and expectation by \mathbb{E} . Additionally, \mathbb{N}_+ denotes the set of all positive integers.

TABLE II
COMPARISON OF SOME RELATED WORKS ON COMPOSITE OPTIMIZATION OR DATA HETEROGENEITY.

Methods	Optimization Can Be		Proximal	Robust to Data	Simple	Linear Rate
	Composite?	Non-convex?	Efficiency?	Heterogeneity?	Subproblems?	Condition
FedAvg-M [21]	✗	✓	✗	✓	✓	✗
SCAFFOLD [19]	✗	✓	✗	✓	✓	Strong Convexity
ProxSkip [14]	✓	✗	✓	-	✓	Strong Convexity
SCAFFNEW [14]	✗	✗	✗	✓	✓	Strong Convexity
FedMiD/FedDA [8]	✓	✗	✗	✗	✓	✗
Fast-FedDA [4]	✓	✗	✗	✗	✓	✗
ZA1 [13]	✓	✗	✗	✓	✓	Strong Convexity
FedPD [25]	✗	✓	✗	✓	✗	✗
FedDC [26]	✗	✓	✗	✓	✗	✗
FedDyn [24]	✗	✓	✗	✓	✗	Strong Convexity
FedDR [27]	✓	✓	✓	✓	✗	✗
FedADMM [28]	✓	✓	✓	✓	✗	✗
FedCanon in This Paper	✓	✓	✓	✓	✓	PL Condition

II. RELATED WORKS

To highlight the main features of this paper, we present a comparison of related works in TABLE II.

SCAFFOLD [19] is a classic FL algorithm that mitigates data heterogeneity by introducing control variables containing global gradient information, eliminating the need for bounded heterogeneity assumptions. However, maintaining control variables on both the server and clients doubles its communication cost compared with FedAvg. Recent work [21] extends FedAvg and SCAFFOLD by incorporating momentums (denoted as FedAvg-M and SCAFFOLD-M, respectively). It has been demonstrated that FedAvg-M could also eliminate bounded heterogeneity assumptions, while SCAFFOLD-M achieves faster convergence rate. Other methods, such as FedProx [29], FedDyn [24], FedPD [25], FedDC [26], mitigate data heterogeneity by local penalty terms. Although these methods are effective in reducing bias between local and global models, they may slow convergence [18]. Moreover, bounded heterogeneity assumptions are still required for convergence analysis of FedProx, FedDC and FedPD.

Research on composite FL is still limited. Previous works [4], [8] also rely on bounded heterogeneity assumptions, while [13] employs SCAFFOLD-like techniques to address both composite optimization and data heterogeneity. However, the convergence analyses in [4], [13], [14] rely on strong convexity assumptions, which restrict their applicability to non-convex problems commonly encountered in neural network training. Furthermore, as discussed earlier, these methods require multiple proximal operations in local updates per iteration, significantly increasing computational burden.

The primal-dual methods, FedDR [27] and FedADMM [28], appear to address challenges related to both data heterogeneity and proximal mapping computations. By leveraging the augmented Lagrangian, these methods decompose primal variables for the loss function and regularization term into client-maintained local variables and server-maintained global variables, efficiently exploiting the structure of composite optimization problems. However, similar to aforementioned works like FedDC, FedPD and FedDyn, as well as other ADMM-

related works like [30], [31], these methods typically require clients to solve subproblems to high accuracy. While they do not impose specific restrictions on the method used to solve the subproblems, the resulting errors can directly impact the overall accuracy. Balancing the trade-off between the accuracy of subproblem solutions and algorithmic efficiency remains a critical issue for these methods in real-world applications.

III. PROPOSED ALGORITHM

In this section, we will first present the problem formulation along with some necessary assumptions, followed by a detailed explanation of the construction process and related discussions of the proposed FedCanon.

A. Problem Formulation

We consider the composite optimization problem in FL of the following form:

$$\min_{\{x_i\}_{i=1}^N, z} \frac{1}{N} \sum_{i \in [N]} f_i(x_i) + h(z), \text{ s.t. } x_i = z, \forall i \in [N], \quad (4)$$

where $x_i \in \mathbb{R}^d, i \in [N]$ are local copies of the global variable $z \in \mathbb{R}^d$. Fundamentally, (4) is equivalent to (1) due to the consensus constraint. The local loss function $f_i(x_i) := \mathbb{E}_{\xi_i \sim \mathcal{D}_i} [F_i(x_i; \xi_i)]$ is a smooth, potentially non-convex function, where ξ_i is an independent sample drawn from the local data distribution \mathcal{D}_i of client i . No extra assumptions are made on the similarity of local data distributions, which highlights the presence of data heterogeneity. The function f can capture a wide range of functions commonly used in neural networks, such as the sigmoid activation function, while h represents a possibly non-smooth regularization term (e.g., ℓ_1 norm, MCP, SCAD penalty) or an indicator function over a closed and compact set.

We now provide more detailed assumptions below.

Assumption 1. The objective function ϕ is lower bounded, i.e., $\phi^* = \inf_z \phi(z) > -\infty$.

Assumption 2. The local function $f_i : \mathbb{R}^d \mapsto \mathbb{R}$ is L -smooth, i.e., for any $x, y \in \mathbb{R}^d$, there exists $L > 0$ such that

$$f_i(x) - f_i(y) - \langle \nabla f_i(y), x - y \rangle \leq \frac{L}{2} \|x - y\|^2, \quad (5a)$$

$$\|\nabla f_i(x) - \nabla f_i(y)\| \leq L \|x - y\|. \quad (5b)$$

Assumptions 1 and 2 are standard conditions commonly adopted in the convergence analysis for non-convex optimization [25], [27]. The smoothness condition in Assumption 2 is weaker than the sample-wise smoothness condition required in [7], [16], [21], [32].

Assumption 3. The function $h : \mathbb{R}^d \rightarrow \mathbb{R} \cup \{+\infty\}$ is proper, closed and ρ -weakly convex (i.e., $h(z) + \frac{\rho}{2} \|z\|^2$ is convex with $\rho \geq 0$), but not necessarily to be smooth. It typically represents a regularization term scaled by a factor $\kappa > 0$. Moreover, for any $h'(z) \in \partial h(z)$, there exists a constant $B_h = \mathcal{O}(\kappa)$ such that $\|h'(z)\|^2 \leq B_h$.

Weak convexity generalizes standard convexity, reducing to it when $\rho = 0$. Although weakly convex functions are non-convex, they retain several valuable properties of convex functions (see Lemma 5 for details). For instance, the proximal operator $\text{prox}_{\alpha h}$ remains applicable to weakly convex functions, provided that $0 < \alpha < 1/\rho$. Common examples of weakly convex regularization terms include MCP and SCAD penalty, which possess bounded subgradients and may outperform ℓ_1 norm in certain machine learning tasks [33], [34]. A broader class of regularization terms with bounded subgradients is discussed in [35]. In practice, these regularization terms are typically scaled by a factor, denoted as κ , to appropriately balance their influence. For example, when employing the ℓ_1 norm, we have $h(z) = \kappa \|z\|_1$ with $B_h = \kappa$. In the training of large-scale models, κ is often chosen to be small in order to mitigate instability during optimization. Compared to existing works that typically assume convex regularization terms, e.g., [8], [13], [32], [34], Assumption 3 is more general and easily satisfied, thereby broadening the applicability of algorithm.

Assumption 4. If $\{\xi_{i,b}\}_{b=1}^B$ are independent samples from \mathcal{D}_i with $B \in \mathbb{N}_+$, the local stochastic gradient estimator $g_i(x_i) := \frac{1}{B} \sum_{b=1}^B \nabla F_i(x_i; \xi_{i,b})$ satisfies [7]:

$$\mathbb{E}[g_i(x_i)] = \nabla f_i(x_i), \quad (6a)$$

$$\mathbb{E}\|g_i(x_i) - \nabla f_i(x_i)\|^2 \leq \sigma^2/B. \quad (6b)$$

Due to limited computational resources of devices, clients in FL typically use unbiased and variance-bounded stochastic gradients instead of the true gradients for large-scale training tasks. To further reduce the variance, we employ the above stochastic gradient estimator based on batch samplings.

In addition to these, many FL-related works also introduce bounded heterogeneity assumptions. These assumptions typically require a certain relationship between global and local gradients¹, which can take the following forms [8], [22], [36]:

$$\max_{j \in [N]} \|\nabla f_j(x)\|^2 \leq \zeta^2; \quad \frac{1}{N} \sum_{j \in [N]} \|\nabla f(x) - \nabla f_j(x)\|^2 \leq \zeta^2;$$

¹Although the first condition only requires the maximum local gradient to be bounded, it implies $\|\nabla f(x)\|^2 = \|\frac{1}{N} \sum_{j \in [N]} \nabla f_j(x)\|^2 \leq \frac{1}{N} \sum_{j \in [N]} \|\nabla f_j(x)\|^2 \leq \zeta^2$. This implies that the bounded gradient assumptions can be viewed as special cases of bounded heterogeneity assumptions.

Algorithm 1 FedCanon

Input: Step size parameters $\alpha, \beta > 0$, number of iterations $T \geq 1$, number of local updates $K \geq 1$, initial global variable $z^0 \in \mathbb{R}^d$, initial control variables $\{c_i^0\}_{i \in [N]} \in \mathbb{R}^d$ with $\sum_{i \in [N]} c_i^0 = \mathbf{0}_d$.
for $t = 0, 1, \dots, T - 1$ **do**

On Client $i \in [N]$ in Parallel Do

Set $\hat{x}_i^{t,0} = z^t$.
for $k = 0, 1, \dots, K - 1$ **do**
 Update $\hat{x}_i^{t,k+1} = \hat{x}_i^{t,k} - \beta [g_i(\hat{x}_i^{t,k}) + c_i^t]$.
end for
 Send $\Delta_i^{t+1} = \frac{1}{\beta K} (z^t - \hat{x}_i^{t,K})$ to server.
 Receive $(\bar{\Delta}^{t+1}, z^{t+1})$ from server.
 Update $c_i^{t+1} = c_i^t + \bar{\Delta}^{t+1} - \Delta_i^{t+1}$.

On Server Do

Receive Δ_i^{t+1} from all clients.
 Update $\bar{\Delta}^{t+1} = \frac{1}{N} \sum_{i \in [N]} \Delta_i^{t+1}$.
 Update $z^{t+1} = \text{prox}_{\alpha h}\{z^t - \alpha \bar{\Delta}^{t+1}\}$.
 Broadcast $(\bar{\Delta}^{t+1}, z^{t+1})$ to all clients.

end for

$$\frac{1}{N} \sum_{j \in [N]} \|\nabla f_j(x)\|^2 \leq \tau^2 \|\nabla f(x)\|^2 + \zeta^2.$$

In contrast, the proposed FedCanon in this paper does not require any such assumptions.

B. Algorithm Development

The complete procedure of FedCanon is outlined in Algorithm 1. This algorithm involves T rounds of communications between clients and the server, where each client performing K local updates during each round. To distinguish between the two levels of iteration, superscripts t and k are used to denote global and local iterations, respectively. At initialization, the step sizes α and β , as well as the number of global iterations T and local updates K , are specified. The server initializes the global variable z^0 and broadcasts it to all clients. Each client then initializes its local control variable c_i^0 such that $\sum_{i \in [N]} c_i^0 = \mathbf{0}_d$ (the simplest approach is to set $c_i^0 = \mathbf{0}_d$ for all clients). During the t -th iteration, client i initializes its local model $\hat{x}_i^{t,0}$ using the global model z^t received from the previous round, and then performs K local updates. In each local update, client i computes a batch-sampled stochastic gradient $g_i(\hat{x}_i^{t,k})$ and adjusts it using its local control variable c_i^t to alleviate client drift. After completing K local updates, client i calculates the difference between its initial and updated local model, sending Δ_i^{t+1} to the server. The server aggregates Δ_i^{t+1} from all clients and computes their average $\bar{\Delta}^{t+1}$. Using this aggregated gradient estimate, the server performs a proximal gradient descent step on z^t , yielding the updated global variable z^{t+1} . Finally, the server broadcasts $(\bar{\Delta}^{t+1}, z^{t+1})$ to all clients, enabling them to update their local models and control variables in preparation for the next round.

The main steps of FedCanon are summarized as follows:

$$\hat{x}_i^{t,k+1} = \hat{x}_i^{t,k} - \beta \left[g_i(\hat{x}_i^{t,k}) + c_i^t \right], \quad \hat{x}_i^{t,0} = z^t, \quad (7a)$$

$$\Delta_i^{t+1} = \frac{1}{\beta K} \left(z^t - \hat{x}_i^{t,K} \right) = v_i^t + c_i^t, \quad (7b)$$

$$\bar{\Delta}^{t+1} = \frac{1}{N} \sum_{j \in [N]} \Delta_j^{t+1} = \bar{v}^t, \quad (7c)$$

$$z^{t+1} = \text{prox}_{\alpha h} \{ z^t - \alpha \bar{\Delta}^{t+1} \}, \quad (7d)$$

$$c_i^{t+1} = c_i^t + \bar{\Delta}^{t+1} - \Delta_i^{t+1} = \bar{v}^t - v_i^t \quad (7e)$$

$$\begin{aligned} &= c_i^t + \frac{1}{\beta N K} \sum_{j \in [N]} \left(z^t - \hat{x}_j^{t,K} \right) - \frac{1}{\beta K} \left(z^t - \hat{x}_i^{t,K} \right) \\ &= c_i^t - \frac{1}{\beta K} \left(\frac{1}{N} \sum_{j \in [N]} \hat{x}_j^{t,K} - \hat{x}_i^{t,K} \right), \end{aligned}$$

where $v_i^t = \frac{1}{K} \sum_{k=0}^{K-1} g_i(\hat{x}_i^{t,k})$ and $\bar{v}^t = \frac{1}{N} \sum_{j \in [N]} v_j^t$. The last equation in (7b) is derived by iterating local updates (7a), while (7c) and (7e) hold due to

$$\frac{1}{N} \sum_{j \in [N]} c_j^{t+1} = \frac{1}{N} \sum_{j \in [N]} c_j^t = \dots = \frac{1}{N} \sum_{j \in [N]} c_j^0 = \mathbf{0}_d.$$

The structure of this algorithm is simple, and follows the general framework of classical algorithms such as FedAvg and SCAFFOLD. However, it is specifically designed to handle more general non-convex composite optimization problems. A key feature of FedCanon is that it delegates the computation of the proximal mapping to the server side, performing this operation only once per communication round, as shown in (7d). This undoubtedly reduces the computational cost significantly, compared with FedMiD and FedDA in [8], ZA1 in [13], particularly in large-scale scenarios with frequent proximal computations on clients.

Compared with SCAFFNEW, Algorithm 1 requires the server to broadcast more variables to all clients in each communication round. To further reduce the number of transmitted variables, modifications can be made such that the proximal mapping step (7d) is performed locally by all clients in parallel, i.e.,

$$\hat{x}_i^{t+1,0} = \text{prox}_{\alpha h} \{ \hat{x}_i^{t,0} - \alpha \bar{\Delta}^{t+1} \}, \quad \forall i \in [N].$$

In this variant, the server is only responsible for aggregating Δ_i and broadcasting $\bar{\Delta}$ to all clients. If all clients are initialized with the same local model, consistency can be maintained at the beginning of each round, without the need to receive the global model, i.e., $\hat{x}_1^{t,0} = \dots = \hat{x}_N^{t,0} = z^t$. We refer to this modified version as **FedCanon II**, and its detailed steps are provided in Algorithm 2. The communication cost of FedCanon II is comparable to that of SCAFFNEW, requiring only two variables to be exchanged between the server and each client per iteration. However, this reduction in communication cost comes at the expense of increased computational burdens: the number of proximal mappings per iteration increases to N , as each client independently performs this step. It demonstrates a trade-off between communication and computation, which should be evaluated based on the computational capabilities of clients and the bandwidth limitations in specific deployment scenarios. TABLE III compares the two versions of FedCanon with several existing composite FL methods, reporting the

Algorithm 2 FedCanon II

Input: Step size parameters $\alpha, \beta > 0$, number of iterations $T \geq 1$, number of local updates $K \geq 1$, initial variables $\hat{x}_1^{0,0} = \dots = \hat{x}_N^{0,0} \in \mathbb{R}^d$, initial control variables $\{c_i^0\}_{i \in [N]} \in \mathbb{R}^d$ with $\sum_{i \in [N]} c_i^0 = \mathbf{0}_d$.
for $t = 0, 1, \dots, T-1$ **do**

On Client $i \in [N]$ in Parallel Do

for $k = 0, 1, \dots, K-1$ **do**

Update $\hat{x}_i^{t,k+1} = \hat{x}_i^{t,k} - \beta \left[g_i^t(\hat{x}_i^{t,k}) + c_i^t \right]$.

end for

Send $\Delta_i^{t+1} = \frac{1}{\beta K} (\hat{x}_i^{t,0} - \hat{x}_i^{t,K})$ to server.

Receive $\bar{\Delta}^{t+1}$ from server.

Update $\hat{x}_i^{t+1,0} = \text{prox}_{\alpha h} \{ \hat{x}_i^{t,0} - \alpha \bar{\Delta}^{t+1} \}$.

Update $c_i^{t+1} = c_i^t + \bar{\Delta}^{t+1} - \Delta_i^{t+1}$.

On Server Do

Receive Δ_i^{t+1} from all clients.

Broadcast $\bar{\Delta}^{t+1} = \frac{1}{N} \sum_{i \in [N]} \Delta_i^{t+1}$ to clients.

end for

total number of proximal operations and the floats exchanged during communication per iteration. Notably, when the number of local updates K is large, FedCanon II still preserves the advantage of efficient proximal operations, as it avoids multiple proximal computations on clients during local updates.

From a practical standpoint, clients often have more limited computational resources than the server, while server-side broadcasting is relatively efficient and easy to implement. Therefore, the structure of Algorithm 1, which centralizes the proximal operation on the server, is generally better suited for real-world FL applications.

TABLE III
COMPARISON OF COMPOSITE FL METHODS: TOTAL PROXIMAL MAPPINGS AND PER-CLIENT COMMUNICATION PER ITERATION

Methods	Total Proximal Computations	Floats Exchange
FedCanon	1	3d
FedCanon II	N	2d
FedMiD / FedDA	$ S K + 1$	2d
Fast-FedDA	$NK_t + 1$	4d
ZA1	$2NK + 1$	2d

In this table, we set the model dimension for all algorithms as d , where $|S|$ represents the number of sampled clients, and K_t denotes the number of local updates performed in the t -th iteration.

C. Relationship with Other Algorithms

The equation (7e) in FedCanon implies that the control variable c_i encapsulates the previous global gradient information, which helps mitigate client drift caused by the heterogeneity of training data. A similar role of this control variable can be observed in SCAFFOLD [19] and SCAFFNEW [14].

The control variable update in SCAFFOLD has two modes, and the main steps of using Option II in [19, Algorithm 1] are

summarized as

$$\hat{x}_i^{t,k+1} = \hat{x}_i^{t,k} - \beta [g_i(\hat{x}_i^{t,k}) + e^t - e_i^t], \quad \hat{x}_i^{t,0} = z^t, \quad (8a)$$

$$\Delta_i^{t+1} = z^t - \hat{x}_i^{t,K}, \quad (8b)$$

$$\Delta e_i^{t+1} = \frac{1}{\beta K} \Delta_i^{t+1} - e^t, \quad (8c)$$

$$e_i^{t+1} = e_i^t + \Delta e_i^{t+1}, \quad e^0 = \frac{1}{N} \sum_{i \in [N]} e_i^0, \quad (8d)$$

$$z^{t+1} = z^t - \frac{\alpha}{|S|} \sum_{i \in S \subseteq [N]} \Delta_i^{t+1}, \quad (8e)$$

$$e^{t+1} = e^t + \frac{1}{N} \sum_{i \in S} \Delta e_i^{t+1}, \quad (8f)$$

The term $e - e_i$ in (8) essentially serves the same role as c_i in (7a). Specifically, it can be easily inferred from the local update step (8a) that

$$\frac{1}{\beta K} \Delta_i^{t+1} \stackrel{(8b)}{=} \frac{1}{\beta K} (z^t - \hat{x}_i^{t,K}) = v_i^t + e^t - e_i^t,$$

which corresponds to (7b). Then, by setting $S = [N]$, for the local and global control variables in (8d) and (8f), we can infer

$$e_i^{t+1} = e_i^t + \Delta e_i^{t+1} \stackrel{(8c)}{=} e_i^t + \frac{1}{\beta K} \Delta_i^{t+1} - e^t = v_i^t,$$

$$\begin{aligned} e^{t+1} &= e^t + \frac{1}{N} \sum_{i \in [N]} \Delta e_i^{t+1} \stackrel{(8c)}{=} e^t + \frac{1}{N} \sum_{i \in [N]} \left[\frac{1}{\beta K} \Delta_i^{t+1} - e^t \right] \\ &= \bar{v}^t + e^t - \frac{1}{N} \sum_{i \in [N]} e_i^t = \frac{1}{N} \sum_{i \in [N]} e_i^{t+1} - \frac{1}{N} \sum_{i \in [N]} e_i^t + e^t. \end{aligned}$$

Since the initial values of the control variables satisfy $e^0 = \frac{1}{N} \sum_{i \in [N]} e_i^0$, it is straightforward to obtain $e^t = \frac{1}{N} \sum_{i \in [N]} e_i^t$ by the above equation. Consequently,

$$e^{t+1} - e_i^{t+1} = \bar{v}^t - v_i^t, \quad \frac{1}{\beta N K} \sum_{i \in [N]} \Delta_i^{t+1} = \bar{v}^t,$$

are equivalent to (7e) and (7c), respectively.

From the perspective of control variables, FedCanon can be considered as an extension of SCAFFOLD to composite problems. In SCAFFOLD, both the server and clients must maintain and update control variables, resulting in the exchange of four variables per client per iteration. In contrast, FedCanon eliminates server-side control variable, thereby reducing communication overhead to three variables per iteration.

SCAFFNEW is an application of ProxSkip to FL, and its main steps are summarized as:

$$\hat{x}_i^{t+1} = x_i^t - \beta [g_i(x_i^t) + e_i^t], \quad (9a)$$

$$x_i^{t+1} = \begin{cases} \frac{1}{N} \sum_{i \in [N]} \hat{x}_i^{t+1}, & \text{with probability } p, \\ \hat{x}_i^{t+1}, & \text{with probability } 1 - p, \end{cases} \quad (9b)$$

$$e_i^{t+1} = e_i^t - \frac{p}{\beta} (x_i^{t+1} - \hat{x}_i^{t+1}), \quad \sum_{i \in [N]} e_i^0 = \mathbf{0}_d. \quad (9c)$$

SCAFFNEW introduces a small probability p , such that in each iteration, the clients skip communication with this probability and performs only local updates; otherwise, the server aggregates and averages all local models, and then broadcasts the result. If (9) is structured in a two-layer iterative form similar to that of FedCanon II, it can be written as

$$\hat{x}_i^{t,k+1} = \hat{x}_i^{t,k} - \beta [g_i(\hat{x}_i^{t,k}) + e_i^t], \quad \hat{x}_i^{t,0} = \frac{1}{N} \sum_{i \in [N]} \hat{x}_i^{t-1, K_p^{t-1}},$$

$$e_i^{t+1} = e_i^t - \frac{p}{\beta} \left(\frac{1}{N} \sum_{i \in [N]} \hat{x}_i^{t, K_p^t} - \hat{x}_i^{t, K_p^t} \right),$$

where K_p^t denotes the number of local updates in the t -th outer iteration. If p in the second equation above is approximately replaced by $1/K_p^t$, then these two equations correspond to (7a) and (7e), respectively.

ProxSkip is originally developed for composite optimization problems, but is centralized in nature. The aggregation and averaging operation performed by the server in SCAFFNEW corresponds to the proximal mapping when the non-smooth term in ProxSkip is set as an indicator function corresponding to the consensus constraint. This implies that ProxSkip can not apply to the composite FL problem. Moreover, [14] provides the convergence analysis for ProxSkip and SCAFFNEW only in the case where the objective function is strongly convex, which limits their applicability.

IV. CONVERGENCE ANALYSIS

In this section, we will present the convergence rates of FedCanon when solving general non-convex composite optimization problems and those satisfying the PL condition.

We first introduce several commonly used notations for the subsequent analysis. From the update of z^{t+1} (7d), we can express it in an alternative form:

$$z^{t+1} = z^t - \alpha \underbrace{\left(z^t - \mathbf{prox}_{\alpha h} \{ z^t - \alpha \bar{\Delta}^{t+1} \} \right)}_{G^\alpha(z^t, \bar{\Delta}^{t+1})}. \quad (10)$$

It is worth noting that if $\bar{\Delta}^{t+1}$ in $G^\alpha(z^t, \bar{\Delta}^{t+1})$ is replaced by $\nabla f(z^t)$, the resulting expression denotes the proximal gradient:

$$G^\alpha(z^t) \triangleq \frac{1}{\alpha} (z^t - \mathbf{prox}_{\alpha h} \{ z^t - \alpha \nabla f(z^t) \}).$$

It is evident that $G^\alpha(z^*) = \mathbf{0}_d$ is equivalent to

$$\mathbf{0}_d \in \nabla f(z^*) + \partial h(z^*),$$

and we refer z^* as the stationary point. Moreover, $G^\alpha(z)$ would reduce to $\nabla f(z)$ when $h = 0$. Therefore, the proximal gradient can be used as a criterion for measuring convergence in some composite optimization algorithms [11], [37]. Next, for $t = 0, \dots, T-1$, we define the following term:

$$\mathcal{E}^{t+1} = \frac{1}{N} \sum_{i \in [N]} \mathbb{E} \|\nabla f_i(\hat{x}_i^{t+1,0}) - v_i^t - \nabla f(z^{t+1}) + \bar{v}^t\|^2.$$

Then, the subsequent two lemmas all hold for the sequence $\{(\{\hat{x}_i^{t,k}\}_{k=0}^{K-1}, \Delta_i^{t+1}, c_i^{t+1})_{i=1}^N, (\bar{\Delta}^{t+1}, z^{t+1})\}_{t=0}^{T-1}$ generated by (7) (equivalent to Algorithms 1 and 2). Their detailed proofs are provided in Appendices B and C, respectively.

Lemma 1. Suppose that Assumptions 1-4 hold, if $0 < \alpha < \frac{1}{\rho}$ and $\beta^2 \leq \frac{1}{24K(K-1)L^2}$, it has

$$\begin{aligned} & \mathbb{E} [\phi(z^{t+1}) - \phi(z^t)] \\ & \leq - \frac{\alpha - 2(\rho + L)\alpha^2}{4} \mathbb{E} \|G^\alpha(z^t, \bar{\Delta}^{t+1})\|^2 - \frac{\alpha}{8} \mathbb{E} \|G^\alpha(z^t)\|^2 \\ & \quad - \left[\frac{\alpha}{16} - 12(2 + \delta)\alpha\beta^2 K^2 L^2 \right] \mathbb{E} \|\nabla f(z^t)\|^2 + \frac{\alpha B_h}{8} \\ & \quad + 12(2 + \delta)\alpha\beta^2 K^2 L^2 \mathcal{E}^t + \frac{\alpha(2 + \delta)(1 + 3\beta^2 K^3 L^2)\sigma^2}{BK}, \end{aligned} \quad (11)$$

where $\delta = 1/(1 - \alpha\rho)^2$.

Lemma 2. Suppose that Assumptions 1-4 hold, then the following inequality holds:

$$\mathcal{E}^{t+1} \leq 48\beta^2 K^2 L^2 (\mathcal{E}^t + \mathbb{E}\|\nabla f(z^t)\|^2) + 2\alpha^2 L^2 \mathbb{E}\|G^\alpha(z^t, \bar{\Delta}^{t+1})\|^2 + \frac{4\sigma^2(1+3\beta^2 K^3 L^2)}{BK}. \quad (12)$$

Remark 1. In Lemma 1, we apply the inequality

$$-\|G^\alpha(z^t)\|^2 \leq B_h - \frac{1}{2}\|\nabla f(z^t)\|^2$$

to introduce a negative term involving $\mathbb{E}\|\nabla f(z^t)\|^2$, which naturally motivates the inclusion of B_h in Assumption 3. Fortunately, as previously discussed, for many widely used regularization terms, an upper bound on their subgradients can be readily determined. Without Assumption 3, controlling $\mathbb{E}\|\nabla f(z^t)\|^2$ requires more restrictive conditions, such as assuming bounded gradients of the loss function, which is an assumption adopted in certain analyses of FedAvg [20], [23].

A. Convergence Analysis under General Non-Convex Settings

By leveraging Lemmas 1 and 2, it is easy to derive the following Theorem 1 for FedCanon applied to general non-convex composite optimization problems. Specifically, adding $\alpha(\mathcal{E}^{t+1} - \mathcal{E}^t)$ to the left-hand side of (11) and substituting (12) into it, we adjust the parameters α and β such that the coefficients of \mathcal{E}^t , $\mathbb{E}\|\nabla f(z^t)\|^2$ and $\mathbb{E}\|G^\alpha(z^t, \bar{\Delta}^{t+1})\|^2$ on the right-hand side become negative to eliminate these terms. By summing and telescoping the resulting inequalities over $t = 0$ to $T - 1$, simplifying the expression, and taking the average yield (13). The details are presented in Appendix D.

Theorem 1. Suppose that Assumptions 1-4 hold, if $0 < \alpha(\rho + L) + 4\alpha^2 L^2 \leq \frac{1}{2}$ and $192(6 + \delta)\beta^2 K^2 L^2 \leq 1$, for the sequence generated by Algorithms 1 and 2, we have

$$\frac{1}{T} \sum_{t=0}^{T-1} \mathbb{E}\|G^\alpha(z^t)\|^2 \leq \frac{8[\phi(z^0) - \phi^* + \alpha\mathcal{E}^0]}{\alpha T} + \frac{50\sigma^2}{BK} + \frac{\sigma^2}{8B} + B_h. \quad (13)$$

Theorem 1 establishes that when the bound B_h can be scaled by κ , the proximal gradient decreases at a sublinear rate of $\mathcal{O}(1/T)$ until it reaches a steady-state error $\mathcal{O}(\frac{\sigma^2}{BK}) + \mathcal{O}(\frac{\sigma^2}{B}) + \mathcal{O}(\kappa)$, which is primarily determined by the variance of the stochastic gradients and the boundedness of the subgradient of the regularization term. This residual error can be further reduced by increasing the mini-batch size B or decreasing the regularization scaling factor κ within h . If $1/B$ and κ are both set to $\mathcal{O}(1/T)$, then Theorem 1 implies the existence of $0 \leq j < T$ such that $\mathbb{E}\|G^\alpha(z^j)\|^2 \leq \epsilon$, which means FedCanon can obtain an expected ϵ -stationary point with iteration complexity $\mathcal{O}(1/\epsilon)$.

Remark 2. To ensure model accuracy, the scaling factor κ should not be set too large, especially when training deep neural networks with a large number of parameters. According to our empirical observations in the next section, when using ResNet architectures, it is advisable to set κ no greater than $\mathcal{O}(10^{-5})$.

Remark 3. Mega-batches appear to be essential for FedCanon to attain solutions with arbitrary accuracy. While some composite FL methods [4], [8] allow residual errors to be controlled via step size parameters, they typically rely on stronger assumptions, such as (strong) convexity or bounded gradients/heterogeneity. Whether solutions with arbitrary accuracy can be obtained using arbitrary batch sizes in non-convex composite FL settings without assuming bounded heterogeneity, remains an open question. To the best of our knowledge, no existing work has addressed this challenge.

B. Convergence Analysis under the PL Condition

The PL condition is an additional assumption considered in many works for convergence analysis, as it enables linear rate for some non-convex algorithms [37]–[39]. This condition means that every stationary point is a global minimizer, but it is weaker than the μ -strong convexity because the global minimum is not unique. Since this work focuses on composite FL, we provide its more general form.

Assumption 5 ([11]). For any $z \in \mathbb{R}^d$, the objective function ϕ satisfies the more general PL condition with $\mu > 0$, i.e.,

$$\|G^\alpha(z)\|^2 \geq 2\mu[\phi(z) - \phi^*]. \quad (14)$$

In Theorem 2, we present the convergence rate of FedCanon under the additional Assumption 5. The process of deriving (15) is similar to (13). Specifically, adding $\alpha\mathcal{E}^{t+1}$ to the left-hand side of (11) and substituting (12), we leverage the inequality from the PL condition to replace the $\mathbb{E}\|G^\alpha(z^t)\|^2$ term. By adjusting the parameters α and β to eliminate the $\mathbb{E}\|\nabla f(z^t)\|^2$ and $\mathbb{E}\|G^\alpha(z^t, \bar{\Delta}^{t+1})\|^2$ terms and ensuring that the coefficient of \mathcal{E}^t does not exceed $\alpha(1 - \frac{\alpha\mu}{4})$, we iteratively substitute the simplified inequality backward until $t = 0$, which leads to (15). The detailed proof is provided in Appendix E.

Theorem 2. Suppose that Assumptions 1-5 hold, if $0 < \alpha(\rho + L) + 4\alpha^2 L^2 \leq \min\left\{\frac{1}{2}, \frac{4\mu(\rho+L)+64L^2}{\mu^2}\right\}$ and $12(6 + \delta)\beta^2 K^2 L^2 \leq \min\left\{\frac{1}{16}, 1 - \frac{\alpha\mu}{4}\right\}$, for the sequence generated by Algorithms 1 and 2, it holds that

$$\mathbb{E}[\phi(z^T) - \phi^*] + \alpha\mathcal{E}^T \leq \left(1 - \frac{\alpha\mu}{4}\right)^T [\phi(z^0) - \phi^* + \alpha\mathcal{E}^0] + \frac{25\sigma^2}{\mu BK} + \frac{\sigma^2}{16\mu B} + \frac{B_h}{2\mu}. \quad (15)$$

Theorem 2 implies that when the objective function satisfies the PL condition, FedCanon can achieve a linear convergence rate with a residual $\frac{1}{2\mu}$ -times that of (13).

Remark 4. According to (7), the aggregated $\bar{\Delta}$ on the server side does not involve the local step size β , implying that β does not affect the update of the global model. It is also reflected in (13) and (15), and has been confirmed through numerical experiments. In practice, one can simply set $\alpha = \beta K$.

V. NUMERICAL EXPERIMENTS

In this section, we evaluate the convergence and effectiveness of FedCanon under different hyperparameter settings and compare it with other state-of-the-art composite FL methods.

All these experiments are executed on a dedicated computing platform equipped with an Intel® Xeon® Gold 6242R CPU, 512GB of RAM and three NVIDIA Tesla P100 GPUs. The operating system is Ubuntu 20.04, and the software environment dependencies include Python 3.8 and PyTorch 1.13.

A. Experimental Setup

1) *Problems*: We set the local loss function as

$$f_i(x_i) = \frac{1}{m_i} \sum_{j=1}^{m_i} \mathcal{L}(\mathcal{M}(x_i, a_{i,j}), b_{i,j}),$$

where \mathcal{M} represents the model output when given model parameters x_i and sample $a_{i,j}$, \mathcal{L} represents the cross-entropy loss between $\mathcal{M}(x_i, a_{i,j})$ and the label $b_{i,j}$. Meanwhile, the regularization term h is set to ℓ_1 -norm, MCP or SCAD penalty. Unless specified, we default to using train loss and test accuracy to illustrate the performance of algorithms.

2) *Datasets*: We employ A9A, MNIST, Fashion MNIST (FMNIST), and CIFAR-10 datasets for the experiments. Model training and accuracy testing are conducted using the pre-split training and test sets from each dataset. These datasets are widely used in the fields of distributed optimization and machine learning, with details summarized in TABLE IV.

3) *Partitions*: To investigate the impact of data heterogeneity, we adopt the strategy in [40] to simulate non-i.i.d. (independent and identically distributed) data across clients, which is activated by sampling from a Dirichlet distribution to induce label skew. Specifically, we sample from $p_k = \text{Dir}(\eta)$ and allocate a proportion p_{ki} of class k samples to client i . Here, $\text{Dir}(\eta)$ quantifies the degree of data heterogeneity with concentration parameter $\eta > 0$. Smaller η indicates stronger heterogeneity, while i.i.d. corresponds to an infinite parameter.

4) *Models*: We assess the algorithmic performance of four models: Linear, MLP, CNN, and ResNet-18 [41]. The Linear model represents a simple linear architecture. The Multilayer Perceptron (MLP) model consists of three linear layers, each followed by a ReLU activation function. To achieve better performance on image data, we employ a convolutional neural network (CNN), which includes two convolutional layers, each followed by a ReLU activation function and a max-pooling layer. ResNet-18, a more complex yet powerful model, is used for further experiments. TABLE V presents the parameter quantities of the employed models across different datasets.

5) *Algorithms*: We select FedAvg, SCAFFOLD [19], SCAFFNEW [14], FedMiD [8], FedDA [8], ZA1 [13], FedDR [27] and FedADMM [28] as the baseline algorithms for comparison with FedCanon.

TABLE IV
AN OVERVIEW OF THE EMPLOYED DATASETS.

Datasets	Train / Test Samples	Classes	Input Size
A9A	32,561 / 16,281	2	123
MNIST / FMNIST	60,000 / 10,000	10	1×28×28
CIFAR-10	50,000 / 10,000	10	3×32×32

B. Experimental Results

Typically, the choice of step size parameters directly influences the convergence rate of FL methods. To investigate

TABLE V
NUMBER OF MODEL PARAMETERS ACROSS DIFFERENT DATASETS.

Models	on A9A	on MNIST / FMNIST	on CIFAR-10
Linear	248	7,850	30,730
MLP	24,258	109,386	402,250
CNN	-	268,362	268,650
ResNet-18	-	11,175,370	11,181,642

A9A is not an image dataset, making it unsuitable for CNN and ResNet-18.

this effect, we uniformly distribute the A9A dataset across 10 clients to train a simple linear model for a binary classification task, with MCP used as the regularization term. By fixing other parameters, we plot the training loss and proximal gradient trajectories of FedCanon under various combinations of α and β in Fig. 1. It can be observed that increasing α appropriately, while keeping β fixed, leads to a faster decrease in training loss and proximal gradient. In contrast, adjusting β while fixing α has a negligible influence on the convergence rate. This is because the information aggregated at the server in FedCanon is scaled by the local step size β .

For a smooth objective problem (i.e., $h = 0$), we compare FedCanon with FedAvg, SCAFFOLD and SCAFFNEW. For all these algorithms, we set the same number of clients, learning rate, local update steps, and training epochs. The FMNIST dataset is used to train an MLP model under three different label distribution settings: i.i.d., weak heterogeneity ($\text{Dir}(0.1)$), and strong heterogeneity ($\text{Dir}(0.01)$). The results are presented in Fig. 2. In the i.i.d. case (Fig. 2 (a)), all algorithms achieve similar performance. Under increasing heterogeneity (Fig. 2 (b) and (c)), FedAvg shows noticeable degradation, with test accuracy dropping by approximately 2% and 10%, respectively, compared to the other algorithms. In contrast, FedCanon, SCAFFOLD, and SCAFFNEW maintain comparable performance and effectively alleviate the impact of data heterogeneity.

TABLE VI
TOTAL COMPUTATION TIME (SECONDS) FOR DIFFERENT ALGORITHMS AND LOCAL UPDATE STEPS K WITH FIXED COMMUNICATION ROUNDS $T = 200$.

K	FedCanon	FedMiD	FedDA	ZA1
10	230	662 ×2.87	804 ×3.49	1106 ×4.80
20	293	1132 ×1.27	1281 ×3.86 ×1.71	2048 ×4.37 ×1.59
40	417	2364 ×6.99 ×1.85	2230 ×5.35 ×1.74	4062 ×9.74 ×1.98
80	719	3875 ×1.42	4126 ×5.67 ×2.09	7201 ×5.35 ×1.74
				×10.02 ×1.77

The values in BLUE indicate the time ratio of each algorithm relative to FedCanon (first column) under the same K setting, while the values in RED represent the time ratio relative to the same algorithm in the previous row.

Next, we compare FedCanon with several existing composite FL methods, including FedMiD, FedDA and ZA1, under different data distributions (i.i.d., $\text{Dir}(1)$ and $\text{Dir}(0.2)$), using the same number of communication rounds ($T = 200$). The FMNIST dataset is partitioned across 10 clients to train a CNN model with the SCAD penalty. Fig. 3 illustrates

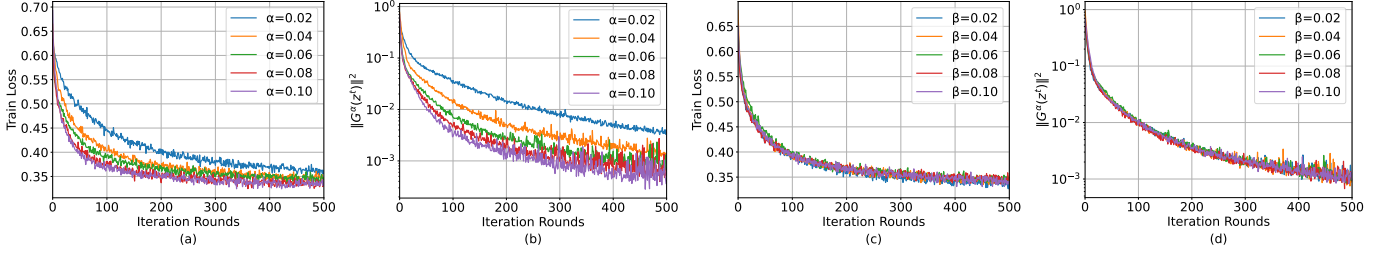


Fig. 1. Training loss and proximal gradient variations of FedCanon under different global and local step sizes α and β : (a) and (b) use the same $\beta = 0.02$ while varying α ; (c) and (d) use the same $\alpha = 0.05$ while varying β .

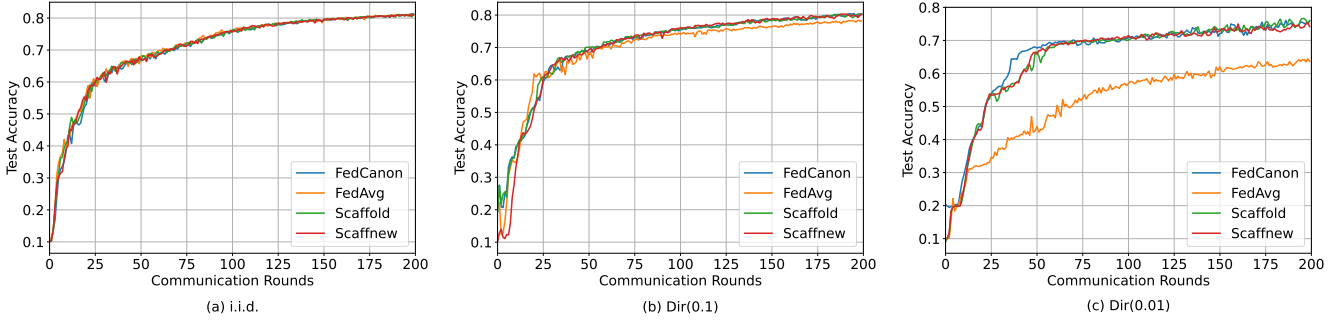


Fig. 2. Performance of FedCanon, FedAvg, SCAFFOLD and SCAFFNEW under different levels of data heterogeneity.

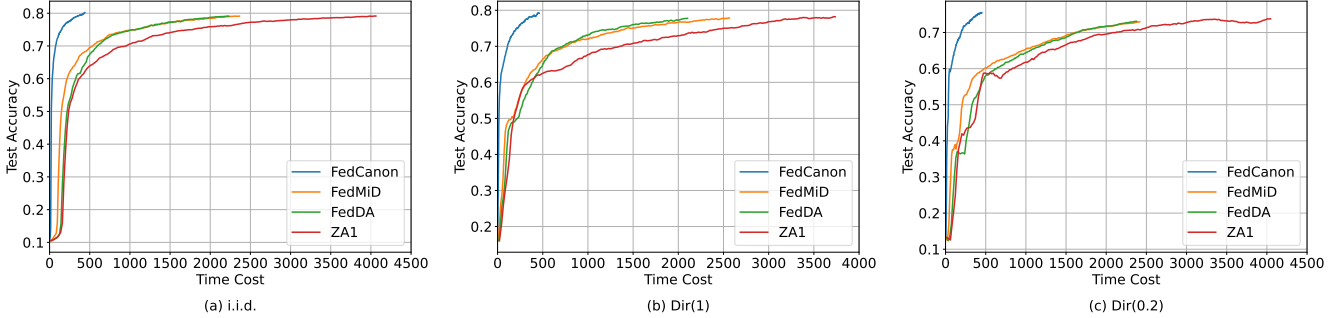


Fig. 3. Test accuracy variations over training time (seconds) for FedCanon, FedMid, FedDA and ZA1, under different levels of data heterogeneity.

the test accuracy over training time for different algorithms with a fixed number of local updates ($K = 40$). Further, TABLE VI provides a more detailed comparison of the training time under the i.i.d. setting for varying local update steps ($K = 10, 20, 40, 80$). As a representative example, the value in the third row and second column indicates that, when $K = 40$, FedMiD consumes 5.67 times more computation than FedCanon, and 2.09 times more than when $K = 20$. Notably, for the same number of communication rounds, FedCanon achieves superior test accuracy while requiring less training time. This advantage is attributed to its efficient algorithmic structure and reduced local computation, underscoring its suitability for composite optimization in heterogeneous data settings.

Additionally, we provide a comparison of the test accuracy after 600 training epochs for FedCanon, FedDR, and FedADMM across different combinations of datasets, models, and data distributions. For the two primal-dual algorithms, each client approximately solves the local subproblem using stochastic gradient descent. The results are summarized in TABLE VII, where each row shows the highest test accuracy achieved across multiple runs for each method under the same model, dataset, and data distribution. As shown, FedCanon achieves the most competitive performance overall.

VI. CONCLUSION

In this paper, we propose a novel composite FL algorithm, FedCanon, designed to address optimization problems composed of potentially non-convex loss functions and weakly convex, possibly non-smooth regularization terms. By incorporating control variables containing global gradient information into local client updates, FedCanon mitigates the adverse effects of data heterogeneity. Additionally, by decoupling the regularization term from the local loss function at the client level, it delegates the computation of proximal mappings solely to the server, thereby significantly reducing the overall computational burden. Theoretical analysis establishes that the algorithm achieves sublinear convergence for general non-convex settings and linear convergence under the PL condition. Numerical experiments further validate its effectiveness. In future work, we plan to integrate FedCanon with advanced security mechanisms, such as privacy preservation and Byzantine fault tolerance [42], to enhance its robustness.

APPENDIX A TECHNICAL LEMMAS

Lemma 3. For any $x, y \in \mathbb{R}^d$, it holds that

$$\langle x/\sqrt{\eta}, \sqrt{\eta}y \rangle \leq \frac{1}{2\eta} \|x\|^2 + \frac{\eta}{2} \|y\|^2, \quad \forall \eta > 0, \quad (16a)$$

TABLE VII
TEST ACCURACY OF FEDCANON, FEDDR, AND FEDADMM ACROSS
DIFFERENT DATASETS, MODELS AND DATA DISTRIBUTIONS.

Datasets	Models	Partitions	FedCanon	FedDR	FedADMM
MNIST	Linear	<i>i.i.d.</i>	0.9039	0.8752	0.8751
		<i>Dir</i> (1)	0.9028	0.8744	0.8743
		<i>Dir</i> (0.2)	0.9018	0.8691	0.8691
	MLP	<i>i.i.d.</i>	0.9229	0.8478	0.8479
		<i>Dir</i> (1)	0.9221	0.8395	0.8427
		<i>Dir</i> (0.2)	0.9218	0.8197	0.8198
FMNIST	CNN	<i>i.i.d.</i>	0.9742	0.8822	0.9172
		<i>Dir</i> (1)	0.9735	0.8622	0.9035
		<i>Dir</i> (0.2)	0.9722	0.8263	0.8655
	MLP	<i>i.i.d.</i>	0.8291	0.7056	0.7085
		<i>Dir</i> (1)	0.8266	0.6908	0.7080
		<i>Dir</i> (0.2)	0.8255	0.6794	0.7052
CIFAR-10	CNN	<i>i.i.d.</i>	0.8510	0.7529	0.7751
		<i>Dir</i> (1)	0.8449	0.7233	0.7335
		<i>Dir</i> (0.2)	0.8355	0.7033	0.7161
	ResNet-18	<i>i.i.d.</i>	0.8791	0.8784	0.8765
		<i>Dir</i> (1)	0.8743	0.8709	0.8700
		<i>Dir</i> (0.2)	0.8513	0.8442	0.8415
CIFAR-100	CNN	<i>i.i.d.</i>	0.5299	0.3100	0.3207
		<i>Dir</i> (1)	0.5241	0.2791	0.3144
		<i>Dir</i> (0.2)	0.4150	0.2183	0.2525
	ResNet-18	<i>i.i.d.</i>	0.5695	0.5248	0.5174
		<i>Dir</i> (1)	0.5183	0.5181	0.5070
		<i>Dir</i> (0.2)	0.4815	0.4812	0.4699

$$\|x + y\|^2 \leq (1 + \eta)\|x\|^2 + (1 + \eta^{-1})\|y\|^2, \quad \forall \eta > 0, \quad (16b)$$

$$-\|x\|^2 \leq \|x - y\|^2 - \frac{1}{2}\|y\|^2. \quad (16c)$$

Lemma 4. For any $x_i \in \mathbb{R}^d$ and $i \in [N]$, it holds that

$$\left\| \sum_{i \in [N]} x_i \right\|^2 \leq N \sum_{i \in [N]} \|x_i\|^2, \quad (17a)$$

$$\sum_{i \in [N]} \|x_i - \bar{x}\|^2 \leq \sum_{i \in [N]} \|x_i\|^2, \quad \bar{x} := \frac{1}{N} \sum_{i \in [N]} x_i. \quad (17b)$$

Lemma 5 ([43]). For any $x, y \in \mathbb{R}^d$, $1 > \tau\rho \geq 0$ and $\tau > 0$, a proper, closed and ρ -weakly convex function $h : \mathbb{R}^d \rightarrow \mathbb{R} \cup \{+\infty\}$ satisfies

$$h(y) \leq h(x) + \langle h'(y), y - x \rangle + \frac{\rho}{2}\|y - x\|^2, \quad (18a)$$

$$\|\text{prox}_{\tau h}\{x\} - \text{prox}_{\tau h}\{y\}\| \leq \frac{1}{1 - \tau\rho}\|x - y\|, \quad (18b)$$

where $h'(y) \in \partial h(y)$.

Lemma 6 ([19]). If the sequence $\{X_1, \dots, X_K\} \subset \mathbb{R}^d$ is Markovian, such that the conditional expectation satisfies $\mathbb{E}[X_k | X_{k-1}, \dots, X_1] = x_k$, and the conditional variance satisfies $\mathbb{E}[\|X_k - x_k\|^2 | x_k] \leq \sigma^2$, then $\{X_k - x_k\}$ forms a martingale. Then, we have the following bound:

$$\mathbb{E} \left\| \sum_{k \in [K]} X_k \right\|^2 \leq 2\mathbb{E} \left\| \sum_{k \in [K]} x_k \right\|^2 + 2K\sigma^2.$$

APPENDIX B PROOF OF LEMMA 1

By directly substituting the definition of the proximal operator to (10), it follows that

$$\begin{aligned} z^{t+1} &= \text{prox}_{\alpha h}\{z^t - \alpha \bar{\Delta}^{t+1}\} \\ &= \arg \min_z \{h(z) + \frac{1}{2\alpha}\|z - (z^t - \alpha \bar{\Delta}^{t+1})\|^2\}. \end{aligned}$$

Using the optimality condition of this minimization problem, we can derive the subgradient:

$$-\frac{1}{\alpha}(z^{t+1} - z^t) - \bar{\Delta}^{t+1} = h'(z^{t+1}) \in \partial h(z^{t+1}).$$

Next, by applying (18a) in Lemma 5 and substituting this subgradient, we can obtain

$$\begin{aligned} h(z^{t+1}) &\leq h(z^t) + \langle h'(z^{t+1}), z^{t+1} - z^t \rangle + \frac{\rho}{2}\|z^{t+1} - z^t\|^2 \\ &= h(z^t) + \left\langle -\frac{1}{\alpha}(z^{t+1} - z^t) - \bar{\Delta}^{t+1}, z^{t+1} - z^t \right\rangle \\ &\quad + \frac{\rho}{2}\|z^{t+1} - z^t\|^2 \\ &= h(z^t) - \langle \bar{\Delta}^{t+1}, z^{t+1} - z^t \rangle - \frac{2 - \alpha\rho}{2\alpha}\|z^{t+1} - z^t\|^2. \quad (19) \end{aligned}$$

Furthermore, since f is L -smooth, it directly follows from (5a) that

$$f(z^{t+1}) \leq f(z^t) + \langle \nabla f(z^t), z^{t+1} - z^t \rangle + \frac{L}{2}\|z^{t+1} - z^t\|^2. \quad (20)$$

Combining (19) and (20), then substituting (10), we obtain

$$\begin{aligned} \phi(z^{t+1}) - \phi(z^t) &= f(z^{t+1}) - f(z^t) + h(z^{t+1}) - h(z^t) \\ &\stackrel{(10)}{\leq} \alpha \langle \bar{\Delta}^{t+1} - \nabla f(z^t), G^\alpha(z^t, \bar{\Delta}^{t+1}) \rangle \\ &\quad - \frac{2\alpha - (\rho + L)\alpha^2}{2}\|G^\alpha(z^t, \bar{\Delta}^{t+1})\|^2 \\ &\stackrel{(16a)}{\leq} \alpha \|\bar{\Delta}^{t+1} - \nabla f(z^t)\|^2 - \frac{3\alpha - 2(\rho + L)\alpha^2}{4}\|G^\alpha(z^t, \bar{\Delta}^{t+1})\|^2, \end{aligned} \quad (21)$$

where $\eta = \frac{1}{2}$ is set in (16a). Next, if $1 - \alpha\rho > 0$ holds, we can deduce the following relation between $G^\alpha(z^t, \bar{\Delta}^{t+1})$ and the proximal gradient $G^\alpha(z^t)$:

$$\begin{aligned} &-\|G^\alpha(z^t, \bar{\Delta}^{t+1})\|^2 \\ &\stackrel{(16c)}{\leq} \|G^\alpha(z^t, \bar{\Delta}^{t+1}) - G^\alpha(z^t)\|^2 - \frac{1}{2}\|G^\alpha(z^t)\|^2 \\ &= \left\| \frac{1}{\alpha} \text{prox}_{\alpha h}\{z^t - \alpha \bar{\Delta}^{t+1}\} - \frac{1}{\alpha} \text{prox}_{\alpha h}\{z^t - \alpha \nabla f(z^t)\} \right\|^2 \\ &\quad - \frac{1}{2}\|G^\alpha(z^t)\|^2 \\ &\stackrel{(18b)}{\leq} \frac{1}{(1 - \alpha\rho)^2} \|\bar{\Delta}^{t+1} - \nabla f(z^t)\|^2 - \frac{1}{2}\|G^\alpha(z^t)\|^2. \end{aligned} \quad (22)$$

Similarly, the relationship between the proximal gradient $G^\alpha(z^t)$ and the gradient of loss function $\nabla f(z^t)$ is given by

$$\begin{aligned} &-\|G^\alpha(z^t)\|^2 \stackrel{(16c)}{\leq} \|G^\alpha(z^t) - \nabla f(z^t)\|^2 - \frac{1}{2}\|\nabla f(z^t)\|^2 \\ &\leq \left\| \frac{1}{\alpha}[z^t - \alpha \nabla f(z^t) - \underbrace{\text{prox}_{\alpha h}\{z^t - \alpha \nabla f(z^t)\}}_{z^+}] \right\|^2 - \frac{1}{2}\|\nabla f(z^t)\|^2 \\ &\leq B_h - \frac{1}{2}\|\nabla f(z^t)\|^2, \quad (23) \end{aligned}$$

where the final inequality follows from the optimality condition of the proximal operator

$$-\frac{1}{\alpha}(z^+ - z^t) - \nabla f(z^t) = h'(z^+) \in \partial h(z^+),$$

and the assumption that the subgradients of the regularization term h are bounded. Then, plugging (22) and (23) into (21), it follows that

$$\begin{aligned}
& \phi(z^{t+1}) - \phi(z^t) \\
& \leq \alpha \|\bar{\Delta}^{t+1} - \nabla f(z^t)\|^2 - \frac{\alpha - 2(\rho + L)\alpha^2}{4} \|G^\alpha(z^t, \bar{\Delta}^{t+1})\|^2 \\
& \quad - \frac{\alpha}{2} \|G^\alpha(z^t, \bar{\Delta}^{t+1})\|^2 \\
& \stackrel{(22)}{\leq} \frac{(2+\delta)\alpha}{2} \|\bar{\Delta}^{t+1} - \nabla f(z^t)\|^2 - \frac{\alpha - 2(\rho + L)\alpha^2}{4} \|G^\alpha(z^t, \bar{\Delta}^{t+1})\|^2 \\
& \quad - \frac{\alpha}{4} \|G^\alpha(z^t)\|^2 \\
& \stackrel{(23)}{\leq} \frac{(2+\delta)\alpha}{2} \|\bar{\Delta}^{t+1} - \nabla f(z^t)\|^2 - \frac{\alpha - 2(\rho + L)\alpha^2}{4} \|G^\alpha(z^t, \bar{\Delta}^{t+1})\|^2 \\
& \quad - \frac{\alpha}{8} \|G^\alpha(z^t)\|^2 - \frac{\alpha}{16} \|\nabla f(z^t)\|^2 + \frac{\alpha B_h}{8}. \tag{24}
\end{aligned}$$

Next, we focus on the expectation of the first term on the right-hand side of (24):

$$\begin{aligned}
& \mathbb{E} \|\bar{\Delta}^{t+1} - \nabla f(z^t)\|^2 \stackrel{(7c)}{=} \mathbb{E} \|\bar{v}^t - \nabla f(z^t)\|^2 \\
& = \mathbb{E} \left\| \frac{1}{NK} \sum_{i=1}^N \sum_{k=0}^{K-1} g_i(\hat{x}_i^{t,k}) - \frac{1}{N} \sum_{i=1}^N \nabla f_i(\hat{x}_i^{t,0}) \right\|^2 \\
& \stackrel{(17a)}{\leq} \frac{1}{NK^2} \sum_{i=1}^N \mathbb{E} \left\| \sum_{k=0}^{K-1} [g_i(\hat{x}_i^{t,k}) - \nabla f_i(\hat{x}_i^{t,0})] \right\|^2 \\
& \stackrel{\text{Lemma 6}}{\leq} \frac{2}{NK^2} \sum_{i=1}^N \mathbb{E} \left\| \sum_{k=0}^{K-1} [\nabla f_i(\hat{x}_i^{t,k}) - \nabla f_i(\hat{x}_i^{t,0})] \right\|^2 + \frac{2\sigma^2}{BK} \\
& \stackrel{(5b), (17a)}{\leq} \frac{2L^2}{NK} \sum_{i=1}^N \sum_{k=0}^{K-1} \mathbb{E} \|\hat{x}_i^{t,k} - \hat{x}_i^{t,0}\|^2 + \frac{2\sigma^2}{BK}, \tag{25}
\end{aligned}$$

Moreover, for $\mathbb{E} \|\hat{x}_i^{t,k} - \hat{x}_i^{t,0}\|^2$ in (25), we can derive the following results:

$$\begin{aligned}
& \mathbb{E} \|\hat{x}_i^{t,k} - \hat{x}_i^{t,0}\|^2 \stackrel{(7a)}{=} \mathbb{E} \|\hat{x}_i^{t,k-1} - \hat{x}_i^{t,0} - \beta[g_i(\hat{x}_i^{t,k-1}) + c_i^t]\|^2 \\
& \stackrel{(16b)}{\leq} \frac{K}{K-1} \mathbb{E} \|\hat{x}_i^{t,k-1} - \hat{x}_i^{t,0}\|^2 + \beta^2 K \mathbb{E} \|g_i(\hat{x}_i^{t,k-1}) + c_i^t\|^2 \\
& \stackrel{(6)}{=} \frac{K}{K-1} \mathbb{E} \|\hat{x}_i^{t,k-1} - \hat{x}_i^{t,0}\|^2 \\
& \quad + \beta^2 K \mathbb{E} \|\nabla f_i(\hat{x}_i^{t,k-1}) + c_i^t\|^2 + \frac{\beta^2 K \sigma^2}{B} \\
& \stackrel{(16b)}{\leq} \frac{K}{K-1} \mathbb{E} \|\hat{x}_i^{t,k-1} - \hat{x}_i^{t,0}\|^2 + 2\beta^2 K \mathbb{E} \|\nabla f_i(\hat{x}_i^{t,0}) + c_i^t\|^2 \\
& \quad + 2\beta^2 K \mathbb{E} \|\nabla f_i(\hat{x}_i^{t,k-1}) - \nabla f_i(\hat{x}_i^{t,0})\|^2 + \frac{\beta^2 K \sigma^2}{B} \\
& \stackrel{(5b)}{\leq} \left(\frac{K}{K-1} + 2\beta^2 K L^2 \right) \mathbb{E} \|\hat{x}_i^{t,k-1} - \hat{x}_i^{t,0}\|^2 \\
& \quad + 2\beta^2 K \mathbb{E} \|\nabla f_i(\hat{x}_i^{t,0}) + c_i^t\|^2 + \frac{\beta^2 K \sigma^2}{B} \\
& \stackrel{(a)}{\leq} \beta^2 K \sum_{r=0}^{k-1} \left(\frac{K}{K-1} + 2\beta^2 K L^2 \right)^r \left[2\mathbb{E} \|\nabla f_i(\hat{x}_i^{t,0}) + c_i^t\|^2 + \frac{\sigma^2}{B} \right] \\
& \leq \beta^2 K^2 \left(\frac{K}{K-1} + 2\beta^2 K L^2 \right)^{K-1} \left[2\mathbb{E} \|\nabla f_i(\hat{x}_i^{t,0}) + c_i^t\|^2 + \frac{\sigma^2}{B} \right],
\end{aligned}$$

where (a) is derived by iteratively substituting (7a) back to $\hat{x}_i^{t,0} = z^t$. Furthermore, if $2\beta^2 K L^2 \leq \frac{1}{12(K-1)}$, by leveraging

the property $\lim_{x \rightarrow \infty} (1 + \frac{1}{x} + \frac{1}{12x})^x = e^{1+\frac{1}{12}} < 3$, we can derive another upper bound:

$$\begin{aligned}
& \sum_{i=1}^N \sum_{k=0}^{K-1} \mathbb{E} \|\hat{x}_i^{t,k} - \hat{x}_i^{t,0}\|^2 \tag{26} \\
& \leq 6\beta^2 K^2 \sum_{i=1}^N \sum_{k=0}^{K-1} \mathbb{E} \|\nabla f_i(\hat{x}_i^{t,0}) + c_i^t\|^2 + \frac{3\beta^2 N K^3 \sigma^2}{B} \\
& \stackrel{(7e)}{=} 6\beta^2 K^3 \sum_{i=1}^N \mathbb{E} \|\nabla f_i(\hat{x}_i^{t,0}) - v_i^{t-1} + \bar{v}^{t-1}\|^2 + \frac{3\beta^2 N K^3 \sigma^2}{B} \\
& = 6\beta^2 K^3 \sum_{i=1}^N \mathbb{E} \|\nabla f_i(\hat{x}_i^{t,0}) - v_i^{t-1} - \nabla f(z^t) + \bar{v}^{t-1} + \nabla f(z^t)\|^2 \\
& \quad + \frac{3\beta^2 N K^3 \sigma^2}{B} \\
& \stackrel{(16b)}{\leq} 12\beta^2 N K^3 \mathcal{E}^t + 12\beta^2 N K^3 \mathbb{E} \|\nabla f(z^t)\|^2 + \frac{3\beta^2 N K^3 \sigma^2}{B}.
\end{aligned}$$

Then, by substituting (25), (26) into (24), the desired equation (11) can be obtained:

$$\begin{aligned}
& \mathbb{E}[\phi(z^{t+1}) - \phi(z^t)] \\
& \leq \frac{(2+\delta)\alpha}{2} \mathbb{E} \|\bar{\Delta}^{t+1} - \nabla f(z^t)\|^2 - \frac{\alpha}{8} \mathbb{E} \|G^\alpha(z^t)\|^2 \\
& \quad - \frac{\alpha - 2(\rho + L)\alpha^2}{4} \mathbb{E} \|G^\alpha(z^t, \bar{\Delta}^{t+1})\|^2 - \frac{\alpha}{16} \mathbb{E} \|\nabla f(z^t)\|^2 + \frac{\alpha B_h}{8} \\
& \stackrel{(25)}{\leq} \frac{\alpha(2+\delta)L^2}{NK} \sum_{i=1}^N \sum_{k=0}^{K-1} \mathbb{E} \|\hat{x}_i^{t,k} - \hat{x}_i^{t,0}\|^2 - \frac{\alpha}{8} \mathbb{E} \|G^\alpha(z^t)\|^2 \\
& \quad - \frac{\alpha - 2(\rho + L)\alpha^2}{4} \mathbb{E} \|G^\alpha(z^t, \bar{\Delta}^{t+1})\|^2 - \frac{\alpha}{16} \mathbb{E} \|\nabla f(z^t)\|^2 \\
& \quad + \frac{\alpha(2+\delta)\sigma^2}{KB} + \frac{\alpha B_h}{8} \\
& \stackrel{(26)}{\leq} - \frac{\alpha - 2(\rho + L)\alpha^2}{4} \mathbb{E} \|G^\alpha(z^t, \bar{\Delta}^{t+1})\|^2 - \frac{\alpha}{8} \mathbb{E} \|G^\alpha(z^t)\|^2 \\
& \quad - \left[\frac{\alpha}{16} - 12(2+\delta)\alpha\beta^2 K^2 L^2 \right] \mathbb{E} \|\nabla f(z^t)\|^2 + \frac{\alpha B_h}{8} \\
& \quad + 12(2+\delta)\alpha\beta^2 K^2 L^2 \mathcal{E}^t + \frac{\alpha(2+\delta)(1+3\beta^2 K^3 L^2)\sigma^2}{KB}.
\end{aligned}$$

APPENDIX C PROOF OF LEMMA 2

The detailed derivation of (12) is given as follows:

$$\begin{aligned}
& \mathcal{E}^{t+1} \stackrel{(17b)}{\leq} \frac{1}{N} \sum_{i=1}^N \mathbb{E} \|\nabla f_i(\hat{x}_i^{t+1,0}) - v_i^t\|^2 \\
& \stackrel{(16b)}{\leq} \frac{2}{N} \sum_{i=1}^N \mathbb{E} \|\nabla f_i(\hat{x}_i^{t,0}) - v_i^t\|^2 \\
& \quad + \frac{2}{N} \sum_{i=1}^N \mathbb{E} \|\nabla f_i(\hat{x}_i^{t+1,0}) - \nabla f_i(\hat{x}_i^{t,0})\|^2 \\
& \stackrel{(5b)}{\leq} \frac{2}{N} \sum_{i=1}^N \mathbb{E} \|\nabla f_i(\hat{x}_i^{t,0}) - v_i^t\|^2 + 2L^2 \mathbb{E} \|z^{t+1} - z^t\|^2 \\
& \stackrel{(10)}{=} \frac{2}{N} \sum_{i=1}^N \mathbb{E} \|\nabla f_i(\hat{x}_i^{t,0}) - \frac{1}{K} \sum_{k=0}^{K-1} g_i(\hat{x}_i^{t,k})\|^2 \\
& \quad + 2\alpha^2 L^2 \mathbb{E} \|G^\alpha(z^t, \bar{\Delta}^{t+1})\|^2
\end{aligned}$$

$$\begin{aligned}
&\stackrel{\text{Lemma 6}}{\leq} \frac{4}{N} \sum_{i=1}^N \mathbb{E} \|\nabla f_i(\hat{x}_i^{t,0}) - \frac{1}{K} \sum_{k=0}^{K-1} \nabla f_i(\hat{x}_i^{t,k})\|^2 \\
&\quad + 2\alpha^2 L^2 \mathbb{E} \|G^\alpha(z^t, \bar{\Delta}^{t+1})\|^2 + \frac{4\sigma^2}{BK} \\
&\stackrel{(5b)}{\leq} \frac{4L^2}{NK} \sum_{i=1}^N \sum_{k=0}^{K-1} \mathbb{E} \|\hat{x}_i^{t,k} - \hat{x}_i^{t,0}\|^2 \\
&\quad + 2\alpha^2 L^2 \mathbb{E} \|G^\alpha(z^t, \bar{\Delta}^{t+1})\|^2 + \frac{4\sigma^2}{BK} \\
&\stackrel{(26)}{\leq} 48\beta^2 K^2 L^2 \mathcal{E}^t + 48\beta^2 K^2 L^2 \mathbb{E} \|\nabla f(z^t)\|^2 \\
&\quad + 2\alpha^2 L^2 \mathbb{E} \|G^\alpha(z^t, \bar{\Delta}^{t+1})\|^2 + \frac{4(1 + 3\beta^2 K^3 L^2)\sigma^2}{BK}.
\end{aligned}$$

APPENDIX D PROOF OF THEOREM 1

By combining (11) and (12), we can construct the following inequality:

$$\begin{aligned}
&\mathbb{E}[\phi(z^{t+1}) - \phi(z^t)] + \alpha(\mathcal{E}^{t+1} - \mathcal{E}^t) \\
&\leq -\frac{\alpha}{8} \mathbb{E} \|G^\alpha(z^t)\|^2 - \underbrace{[\alpha - 12(6 + \delta)\alpha\beta^2 K^2 L^2]}_{\geq 0} \mathcal{E}^t \\
&\quad - \underbrace{\left[\frac{\alpha - 2(\rho + L)\alpha^2}{4} - 2\alpha^3 L^2\right]}_{\geq 0} \mathbb{E} \|G^\alpha(z^t, \bar{\Delta}^{t+1})\|^2 \\
&\quad - \underbrace{\left[\frac{\alpha}{16} - 12(6 + \delta)\alpha\beta^2 K^2 L^2\right]}_{\geq 0} \mathbb{E} \|\nabla f(z^t)\|^2 \\
&\quad + \frac{\alpha(6 + \delta)(1 + 3\beta^2 K^3 L^2)\sigma^2}{BK} + \frac{\alpha B_h}{8}.
\end{aligned} \tag{27}$$

To satisfy the requirements for convergence analysis, we need to ensure that the coefficients of the second and third terms on the right-hand side of (27) are negative. Therefore, we can determine a feasible range for α and β :

$$\alpha(\rho + L) + 4\alpha^2 L^2 \leq \frac{1}{2}, \tag{28a}$$

$$\beta^2 \leq \frac{1}{192(6 + \delta)K^2 L^2}. \tag{28b}$$

If the above conditions are satisfied, we can rearrange (27) to obtain

$$\begin{aligned}
&\mathbb{E} \|G^\alpha(z^t)\|^2 \\
&\leq \frac{8}{\alpha} \mathbb{E}[\phi(z^t) - \phi(z^{t+1})] + 8[\mathcal{E}^t - \mathcal{E}^{t+1}] \\
&\quad + \frac{8(6 + \delta)(1 + 3\beta^2 K^3 L^2)\sigma^2}{BK} + B_h \\
&\stackrel{(28)}{\leq} \frac{8}{\alpha} \mathbb{E}[\phi(z^t) - \phi(z^{t+1})] + 8[\mathcal{E}^t - \mathcal{E}^{t+1}] + \frac{50\sigma^2}{BK} + \frac{\sigma^2}{8B} + B_h,
\end{aligned}$$

By summing and telescoping the above inequality from $t = 0$ to $T - 1$, and taking the average, we can derive (13).

APPENDIX E PROOF OF THEOREM 2

If the objective function satisfies the more general PL condition described in Assumption 5, then

$$\|G^\alpha(z^t)\|^2 \geq 2\mu[\phi(z^t) - \phi^*]$$

naturally follows from (14). Subsequently, substituting it directly into (11) yields the following inequality:

$$\begin{aligned}
&\mathbb{E}[\phi(z^{t+1}) - \phi^*] \\
&\leq \left(1 - \frac{\alpha\mu}{4}\right) \mathbb{E}[\phi(z^t) - \phi^*] - \frac{\alpha - 2(\rho + L)\alpha^2}{4} \mathbb{E} \|G^\alpha(z^t, \bar{\Delta}^{t+1})\|^2 \\
&\quad - \frac{\alpha}{16} \mathbb{E} \|\nabla f(z^t)\|^2 + 12(2 + \delta)\alpha\beta^2 K^2 L^2 [\mathcal{E}^t + \mathbb{E} \|\nabla f(z^t)\|^2] \\
&\quad + \frac{\alpha(2 + \delta)(1 + 3\beta^2 N L^2 K^3)\sigma^2}{BK} + \frac{\alpha B_h}{8}.
\end{aligned} \tag{29}$$

Using a similar approach to constructing (27), we combine (12) and (29), which leads to

$$\begin{aligned}
&\mathbb{E}[\phi(z^{t+1}) - \phi^*] + \alpha\mathcal{E}^{t+1} \\
&\leq \underbrace{\left(1 - \frac{\alpha\mu}{4}\right)}_{\in(0,1)} \mathbb{E}[\phi(z^t) - \phi^*] + \underbrace{\alpha[12(6 + \delta)\beta^2 K^2 L^2]}_{\leq(1 - \frac{\alpha\mu}{4})} \mathcal{E}^t \\
&\quad - \underbrace{\left[\frac{\alpha - 2(\rho + L)\alpha^2}{4} - 2\alpha^3 L^2\right]}_{\geq 0} \mathbb{E} \|G^\alpha(z^t, \bar{\Delta}^{t+1})\|^2 \\
&\quad - \underbrace{\left[\frac{\alpha}{16} - 12\alpha(6 + \delta)\beta^2 K^2 L^2\right]}_{\geq 0} \mathbb{E} \|\nabla f(z^t)\|^2 \\
&\quad + \frac{\alpha(6 + \delta)(1 + 3K^3 L^2 \beta^2)\sigma^2}{BK} + \frac{\alpha B_h}{8}.
\end{aligned} \tag{30}$$

Similar to (27), we need to ensure that the coefficients on the right-hand side of (30) satisfy the above conditions. Therefore, the range of values for α and β is expressed as

$$\alpha(\rho + L) + 4\alpha^2 L^2 \leq \min \left\{ \frac{1}{2}, \frac{4\mu(\rho + L) + 64L^2}{\mu^2} \right\}, \tag{31a}$$

$$12(6 + \delta)\beta^2 K^2 L^2 \leq \min \left\{ \frac{1}{16}, 1 - \frac{\alpha\mu}{4} \right\}. \tag{31b}$$

Then, we can simplify (30) to the following form:

$$\begin{aligned}
&\mathbb{E}[\phi(z^{t+1}) - \phi^*] + \alpha\mathcal{E}^{t+1} \\
&\leq \left(1 - \frac{\alpha\mu}{4}\right) [\mathbb{E}[\phi(z^t) - \phi^*] + \alpha\mathcal{E}^t] \\
&\quad + \frac{\alpha(6 + \delta)(1 + 3\beta^2 K^3 L^2)\sigma^2}{BK} + \frac{\alpha B_h}{8}.
\end{aligned}$$

By recursively substituting this inequality, we can derive the desired result in (15):

$$\begin{aligned}
&\mathbb{E}[\phi(z^T) - \phi^*] + \alpha\mathcal{E}^T \\
&\leq \left(1 - \frac{\alpha\mu}{4}\right)^T [\phi(z^0) - \phi^* + \alpha\mathcal{E}^0] \\
&\quad + \left[\sum_{t=0}^{T-1} \left(1 - \frac{\alpha\mu}{4}\right)^t\right] \left[\frac{\alpha\sigma^2(6 + \delta)(1 + 3\beta^2 K^3 L^2)}{BK} + \frac{\alpha B_h}{8}\right] \\
&\leq \left(1 - \frac{\alpha\mu}{4}\right)^T [\phi(z^0) - \phi^* + \alpha\mathcal{E}^0] \\
&\quad + \frac{4(6 + \delta)(1 + 3\beta^2 K^3 L^2)\sigma^2}{\mu BK} + \frac{B_h}{2\mu} \\
&\stackrel{(31)}{\leq} \left(1 - \frac{\alpha\mu}{4}\right)^T [\phi(z^0) - \phi^* + \alpha\mathcal{E}^0] + \frac{25\sigma^2}{\mu BK} + \frac{\sigma^2}{16\mu B} + \frac{B_h}{2\mu},
\end{aligned}$$

where the second inequality is obtained by using the fact that $\sum_{t=0}^{\infty} \gamma^t = \frac{1}{1-\gamma}$, for $\gamma \in (0, 1)$.

REFERENCES

- [1] V. Mothukuri, R. M. Parizi, S. Pouriyeh, Y. Huang, A. Dehghantanha, and G. Srivastava, "A survey on security and privacy of federated learning," *Futur. Gener. Comp. Syst.*, vol. 115, pp. 619–640, 2021.
- [2] W. Huang, M. Ye, Z. Shi, G. Wan, H. Li, B. Du, and Q. Yang, "Federated learning for generalization, robustness, fairness: A survey and benchmark," *IEEE Trans. Pattern Anal. Mach. Intell.*, 2024.
- [3] B. McMahan, E. Moore, D. Ramage, S. Hampson, and B. A. y Arcas, "Communication-efficient learning of deep networks from decentralized data," in *Proc. Int. Conf. Artif. Intell. Statist.*, pp. 1273–1282, PMLR, 2017.
- [4] Y. Bao, M. Crawshaw, S. Luo, and M. Liu, "Fast composite optimization and statistical recovery in federated learning," in *Int. Conf. Machin. Learn., ICML*, pp. 1508–1536, PMLR, 2022.
- [5] P. Kairouz, H. B. McMahan, B. Avent, A. Bellet, M. Bennis, A. N. Bhagoji, K. Bonawitz, Z. Charles, G. Cormode, R. Cummings, et al., "Advances and open problems in federated learning," *Found. Trends Mach. Learn.*, vol. 14, no. 1–2, pp. 1–210, 2021.
- [6] H. Zhu, J. Xu, S. Liu, and Y. Jin, "Federated learning on non-iid data: A survey," *Neurocomputing*, vol. 465, pp. 371–390, 2021.
- [7] R. Xin, S. Das, U. A. Khan, and S. Kar, "A stochastic proximal gradient framework for decentralized non-convex composite optimization: Topology-independent sample complexity and communication efficiency," *arXiv preprint arXiv:2110.01594*, 2021.
- [8] H. Yuan, M. Zaheer, and S. Reddi, "Federated composite optimization," in *Int. Conf. Machin. Learn., ICML*, pp. 12253–12266, PMLR, 2021.
- [9] L. Guo, X. Shi, J. Cao, and Z. Wang, "Decentralized inexact proximal gradient method with network-independent stepsizes for convex composite optimization," *IEEE Trans. Signal Process.*, vol. 71, pp. 786–801, 2023.
- [10] P. L. Combettes and J.-C. Pesquet, "Proximal splitting methods in signal processing," *Fix. Point Algor. Inverse Probl. Sci. Eng.*, pp. 185–212, 2011.
- [11] Z. Li and J. Li, "A simple proximal stochastic gradient method for nonsmooth nonconvex optimization," *Proc. Adv. Neural Inf. Process. Syst., NeurIPS*, vol. 31, 2018.
- [12] E. K. Ryu and W. Yin, *Large-scale convex optimization: algorithms & analyses via monotone operators*. Cambridge University Press, 2022.
- [13] J. Zhang, J. Hu, and M. Johansson, "Composite federated learning with heterogeneous data," in *IEEE Int. Conf. Acoust. Speech Signal Process Proc., ICASSP*, pp. 8946–8950, IEEE, 2024.
- [14] K. Mishchenko, G. Malinovsky, S. Stich, and P. Richtárik, "Proxskip: Yes! Local gradient steps provably lead to communication acceleration! Finally!," in *Int. Conf. Machin. Learn., ICML*, pp. 15750–15769, PMLR, 2022.
- [15] J. Pei, W. Liu, J. Li, L. Wang, and C. Liu, "A review of federated learning methods in heterogeneous scenarios," *IEEE Trans. Consum. Electron.*, vol. 70, no. 3, pp. 5983–5999, 2024.
- [16] Y. Liu, X. Zhang, Y. Kang, L. Li, T. Chen, M. Hong, and Q. Yang, "FedBCD: A communication-efficient collaborative learning framework for distributed features," *IEEE Trans. Signal Process.*, vol. 70, pp. 4277–4290, 2022.
- [17] M. Mendieta, T. Yang, P. Wang, M. Lee, Z. Ding, and C. Chen, "Local learning matters: Rethinking data heterogeneity in federated learning," in *Proc. IEEE Comput. Soc. Conf. Comput. Vision Pattern Recognit, CVPR*, pp. 8397–8406, 2022.
- [18] J. Wang, Q. Liu, H. Liang, G. Joshi, and H. V. Poor, "A novel framework for the analysis and design of heterogeneous federated learning," *IEEE Trans. Signal Process.*, vol. 69, pp. 5234–5249, 2021.
- [19] S. P. Karimireddy, S. Kale, M. Mohri, S. Reddi, S. Stich, and A. T. Suresh, "Scaffold: Stochastic controlled averaging for federated learning," in *Int. Conf. Machin. Learn., ICML*, pp. 5132–5143, PMLR, 2020.
- [20] X. Li, K. Huang, W. Yang, S. Wang, and Z. Zhang, "On the convergence of FedAvg on non-iid data," in *Int. Conf. Learn. Represent., ICLR*, 2020.
- [21] Z. Cheng, X. Huang, P. Wu, and K. Yuan, "Momentum benefits non-iid federated learning simply and provably," in *Int. Conf. Learn. Represent., ICLR*, 2024.
- [22] M. Xiang, S. Ioannidis, E. Yeh, C. Joe-Wong, and L. Su, "Efficient federated learning against heterogeneous and non-stationary client unavailability," in *Proc. Adv. Neural Inf. Process. Syst., NeurIPS*, 2024.
- [23] H. Yu, S. Yang, and S. Zhu, "Parallel restarted with faster convergence and less communication: Demystifying why model averaging works for deep learning," in *Proc. AAAI Conf. Artif. Intell., AAAI*, vol. 33, pp. 5693–5700, 2019.
- [24] A. E. Durmus, Z. Yue, M. Ramon, M. Matthew, W. Paul, and S. Venkatesh, "Federated learning based on dynamic regularization," in *Int. Conf. Learn. Represent., ICLR*, 2021.
- [25] X. Zhang, M. Hong, S. Dhople, W. Yin, and Y. Liu, "FedPD: A federated learning framework with adaptivity to non-iid data," *IEEE Trans. Signal Process.*, vol. 69, pp. 6055–6070, 2021.
- [26] L. Gao, H. Fu, L. Li, Y. Chen, M. Xu, and C.-Z. Xu, "FedDC: Federated learning with non-iid data via local drift decoupling and correction," in *Proc. IEEE Comput. Soc. Conf. Comput. Vision Pattern Recognit, CVPR*, pp. 10112–10121, 2022.
- [27] Q. Tran Dinh, N. H. Pham, D. Phan, and L. Nguyen, "FedDR—randomized Douglas-Rachford splitting algorithms for nonconvex federated composite optimization," *Proc. Adv. Neural Inf. Process. Syst., NeurIPS*, vol. 34, pp. 30326–30338, 2021.
- [28] H. Wang, S. Marella, and J. Anderson, "FedADMM: A federated primal-dual algorithm allowing partial participation," in *Proc. IEEE Conf. Decis. Control, CDC*, pp. 287–294, IEEE, 2022.
- [29] T. Li, A. K. Sahu, M. Zaheer, M. Sanjabi, A. Talwalkar, and V. Smith, "Federated optimization in heterogeneous networks," *Proc. Mach. Learn. Syst.*, vol. 2, pp. 429–450, 2020.
- [30] B. Wang, J. Fang, H. Li, X. Yuan, and Q. Ling, "Confederated learning: Federated learning with decentralized edge servers," *IEEE Trans. Signal Process.*, vol. 71, pp. 248–263, 2023.
- [31] S. Zhou and G. Y. Li, "Federated learning via inexact ADMM," *IEEE Trans. Pattern Anal. Mach. Intell.*, vol. 45, no. 8, pp. 9699–9708, 2023.
- [32] G. Mancino-Ball, S. Miao, Y. Xu, and J. Chen, "Proximal stochastic recursive momentum methods for nonconvex composite decentralized optimization," in *Proc. AAAI Conf. Artif. Intell., AAAI*, vol. 37, pp. 9055–9063, 2023.
- [33] A. Böhm and S. J. Wright, "Variable smoothing for weakly convex composite functions," *J. Optim. Theory Appl.*, vol. 188, pp. 628–649, 2021.
- [34] Y. Yan, J. Chen, P.-Y. Chen, X. Cui, S. Lu, and Y. Xu, "Compressed decentralized proximal stochastic gradient method for nonconvex composite problems with heterogeneous data," in *Int. Conf. Machin. Learn., ICML*, pp. 39035–39061, PMLR, 2023.
- [35] F. Xu, J. Duan, and W. Liu, "Comparative study of non-convex penalties and related algorithms in compressed sensing," *Digit. Signal Process.*, vol. 135, p. 103937, 2023.
- [36] J. Bian, L. Wang, K. Yang, C. Shen, and J. Xu, "Accelerating hybrid federated learning convergence under partial participation," *IEEE Trans. Signal Process.*, 2024.
- [37] Z. Wang, K. Ji, Y. Zhou, Y. Liang, and V. Tarokh, "Spiderboost and momentum: Faster variance reduction algorithms," *Proc. Adv. Neural Inf. Process. Syst., NeurIPS*, vol. 32, 2019.
- [38] H. Karimi, J. Nutini, and M. Schmidt, "Linear convergence of gradient and proximal-gradient methods under the Polyak-Łojasiewicz condition," in *Mach. Learn. Knowl. Discov. Datab., ECML PKDD*, pp. 795–811, Springer, 2016.
- [39] X. Yi, S. Zhang, T. Yang, T. Chai, and K. H. Johansson, "Communication compression for distributed nonconvex optimization," *IEEE Trans. Autom. Control*, vol. 68, no. 9, pp. 5477–5492, 2022.
- [40] M. Ye, X. Fang, B. Du, P. C. Yuen, and D. Tao, "Heterogeneous federated learning: State-of-the-art and research challenges," *ACM Comput. Surv.*, vol. 56, no. 3, pp. 1–44, 2023.
- [41] K. He, X. Zhang, S. Ren, and J. Sun, "Deep residual learning for image recognition," in *Proc. IEEE Comput. Soc. Conf. Comput. Vision Pattern Recognit, CVPR*, pp. 770–778, 2016.
- [42] J. Zhang, X. He, Y. Huang, and Q. Ling, "Byzantine-robust and communication-efficient personalized federated learning," *IEEE Trans. Signal Process.*, 2024.
- [43] S. Chen, A. Garcia, and S. Shahrampour, "On distributed nonconvex optimization: Projected subgradient method for weakly convex problems in networks," *IEEE Trans. Autom. Control*, vol. 67, no. 2, pp. 662–675, 2021.